JOURNAL OF CATALYSIS **158,** 502–510 (1996)
ARTICLE NO. 0049

Reaction of Benzene and Pyridine on Metal-Promoted Sulfated Zirconia Catalysts

Ram Srinivasan,* Robert A. Keogh,* Anca Ghenciu,† Dan Fărcaşiu,† and Burtron H. Davis*

*Center for Applied Energy Research, 3572 Iron Works Pike, Lexington, Kentucky 40511; and †Department of Chemical and Petroleum Engineering, University of Pittsburgh, 1249 Benedum Hall, Pittsburgh, Pennsylvania 15261

Received February 15, 1995; revised September 15, 1995

The reactions of benzene and pyridine on sulfated zirconia (I), 0.6 wt%Pt/SO_4^{2-}/ZrO_2 (II), and 2 wt% Fe/0.5 wt% Mn/SO_4^{2-}/ZrO_2 (III) upon heating between 100 and 800°C in an inert atmosphere were studied with a TG/MS instrument. Benzene was converted to carbon dioxide and coke, whereas most pyridine reacted in the same way, but a minor amount was desorbed unchanged. Sulfur dioxide and oxygen also evolved in all cases. Formation of sulfur dioxide indicates that sulfate is the oxidizing species. The coke was also converted to CO_2 in a second heating cycle, conducted in air, but the solid gained weight in this step, indicating that some of the oxygen consumed for the oxidation of the organic molecules originated in the ZrO_2. These results show that the TPD of very weak (benzene) or even stronger (pyridine) organic bases does not measure the acidity of sulfated zirconia or of composite materials based on it.

INTRODUCTION

Sulfated zirconia catalysts have become a subject of extensive research in heterogeneous catalysis. It was claimed not only that they are superacidic, but that they possess all the four important chemical properties, that is, acidic, basic, reducing, and oxidizing (1). Sulfated zirconia catalysts have been tested for various reactions, but especially reactions normally requiring strong acid catalysts.

Investigating the role of sulfate in this catalyst, Nascimento *et al.* (2) found a correlation of activity for *n*-butane isomerization with the sulfur content. It was concluded that maximum activity requires the presence of both Brønsted and Lewis sites, with the ratio of these two being close to 1, and it was suggested that superacidity of SO_4^{2-}/ZrO_2 catalysts (I) could arise from the enhancement of Brønsted site strength by the presence of strong neighboring Lewis sites.

Sulfated zirconia catalysts containing noble metals, most often platinum, have also been studied (3–7). The noble metal crystallites were considered to enhance greatly the activity and stability of the catalysts (3, 4). The state and role of platinum in these materials are matters of controversy; some opposing views have been presented. Wen *et al.* (4) suggested a bifunctional role of platinum, whereas Ebitani *et al.* (8, 9) considered that platinum induces a promoting effect of hydrogen by dissociation of the latter, which is followed by spillover and generation of strong Brønsted acid sites. Recently, the latter authors showed, on the basis of XPS data, that a Pt/SO_4^{2-}/ZrO_2 catalysts, pretreated with hydrogen at 350°C, scarcely chemisorbed CO molecules and that, in the presence of sulfate ions, platinum remained in an oxidized state after reduction in hydrogen at 400°C (10, 11). Ebitani *et al.* (9) have also suggested that the unique properties of the Pt/SO_4^{2-}/ZrO_2 catalyst (II) arise from the fact that a large fraction of platinum remains as PtO and PtS and the metallic fraction is low. Sayari and Dicko (12), however, reported that metallic Pt was present after activation of this catalyst at 600°C in air, a result confirmed by XAFS measurements on a catalyst which had been heated at 725°C (13). It was proposed that evolution or desorption of SO_2 generated some reducing species which converted ionic platinum to its metallic state.

The nature and concentration of acid sites on Catalysts I and II were evaluated from the IR spectra of adsorbed pyridine (9, 14–16). In one work, it was reported that the molar ratio of acid sites which retain pyridine strongly and sulfate groups on the surface is about 1 : 200 (9). In another study, it was found that the percentage of Brønsted sites increases with the sulfate loading (15). Materials containing 9.87% sulfate (3.29% S, Table 2) before calcination were found to give catalysts containing almost exclusively Brønsted sites if activated at 100°C before pyridine adsorption; activation at 400°C between calcination and pyridine adsorption gave catalysts in which around 60% of sites were Brønsted sites (14). Earlier results of exclusive Lewis sites on a sulfated zirconia had been obtained using a material prepared by sulfation of calcined zirconia rather than of zirconium hydroxide (16). Another important factor is moisture, which converts Lewis sites to Brønsted sites. In contrast to earlier claims (8, 9), addition of Pt (Catalyst II) does not change the Brønsted to Lewis site

0021-9517/96 $12.00

ratio and pretreatment with hydrogen does not make a significant difference, either, for Catalyst II as well as for Catalyst I (14).

Recently, it was discovered that doping sulfated zirconia with Fe and Mn gives catalysts active for skeletal isomerization of butane even at room temperature (17–19). Kinetic measurements indicated that the doped catalysts were about three orders of magnitude more active than sulfated ZrO_2 (17, 18). It was also reported that acidity of these materials could be evaluated by temperature-programmed desorption (TPD) of benzene (18, 20). A significantly higher temperature for desorption was observed for Fe/Mn/SO_4^{2-}/ZrO_2 (III) than for nondoped SO_4^{2-}/ZrO_2 (I), and this was interpreted as demonstrating the greater acid strength of the former, making it an exceptional solid superacid (18).

The use of benzene to measure superacid strength has been demonstrated in solution (21). Only very strong superacids were amenable to measurement with this indicator. For example, only 50% hydronation of benzene was observed in 30 : 1 HF-TaF5 (21), an acid shown later to be nearly 11 orders of magnitude stronger than trifluoromethanesulfonic acid (H_0 −14.2) (22). Complete hydronation was observed only in 4 : 1 HBr–$AlBr_3$ and 30 : 1 HF–SbF_5, but only for a ratio SbF_5:benzene of 3 or more. At ratios of 2 or less, no hydronation occurred. Instead, benzene was converted to a polymer (oxidation), even though the temperature of the experiment was 0°C (21). For the conclusions of the TPD study (18), in which the catalyst was first saturated with benzene then heated, to be valid it was necessary that (a) benzene be fully hydronated by the solid acid at a ratio of acid sites : benzene of 1 or less and (b) hydronated benzene be stable to temperatures above 500°C. The first condition would make Catalyst III a much stronger acid than HF–SbF_5, and the second is highly unlikely because earlier attempts to run laser-Raman spectra of hydronated benzene showed that the heat from the laser beam was sufficient to produce darkening and decomposition of the sample (23).

To understand better the interaction of benzene with Catalyst III, a comparative study of the TPD of benzene and pyridine was conducted (24). If the desorption temperature is determined by the strength of the acid–base interaction, pyridine, a stronger base than benzene by 24–25 orders of magnitude, should desorb at a temperature much higher than that of the latter. In fact, the two bases gave desorption peaks at near-equal temperatures. It appeared, therefore, questionable whether the TPD experiments measured acid–base interactions (24).

In a recently published study (25), the high activity of Catalyst III for butane isomerization was confirmed, but it was also observed that the compounds which desorbed from the catalyst in benzene TPD experiments were a mixture of CO_2, SO_2, and O_2. We report here the results of a systematic study of benzene and pyridine adsorption on III, the parent SO_4^{2-}/ZrO_2 (I), and 0.6%Pt/SO_4^{2-}/ZrO_2 (II), using a simultaneous thermogravimetric analysis (TGA)/mass spectrometry (MS) technique.

EXPERIMENTAL

Zirconia was precipitated rapidly at pH 10.5 by admixing a 0.3 *M* aqueous solution prepared from anhydrous $ZrCl_4$ and an excess (approx three- to fourfold) amount of NH_4OH with vigorous stirring. The resulting precipitate was washed thoroughly with deionized water until it gave negative test for the presence of chloride ions in the wash (26). The precipitate, after drying at 110°C for at least 50 h, contained less than 3 ppm Cl^-. For sulfation, the dried hydroxide gel was immersed in 0.5 *M* H_2SO_4 (15 ml/g of catalyst) and stirred for 2 h, filtered without washing, and dried. The dried sample contained 3.4–3.5 wt% sulfur. The appropriate amounts of Fe(III) and Mn(II) nitrate salts were dissolved in the amount of water needed to prepare a catalyst containing 2 wt% Fe and 0.5 wt% Mn by the incipient wetness technique. After impregnation, all catalysts were dried at 120°C overnight and stored in a desiccator until needed. Catalyst activation was conducted at 725°C for 2 h for Catalysts I and II and at 650°C for 2 h for Catalyst III. These temperatures produced a material with activity for *n*-hexadecane conversion higher than that of materials activated at either higher or lower temperatures.

Differential thermal analysis (DTA), thermogravimetric analysis, and the mass spectrometry of the evolved gases were carried out simultaneously using a Seiko TGA/DTA 320 instrument, which was coupled to a VG micromass quadrupole mass spectrometer. This Seiko instrument has an operating temperature up to 1200°C. The runs were conducted separately in helium, as well as in a mixture of He/H_2 or He/air mixtures. For the runs conducted in helium, a flow rate of 200 ml/min was used. For the runs conducted in the mixture of gases, the helium flow was 150 ml/min from one gas inlet port, and the flow of air was 100 ml/min through another gas inlet port. The first gas inlet port was always used for helium flow, and the second gas inlet port was used for introducing the second gas (H_2, air, etc.). Platinum pans were used as sample holders, and Al_2O_3 was used as the reference material. The TGA unit was connected to a disk station that performs tasks such as programmable heating and cooling cycles, continuous weight measurements, sweep gas valve switching, and data storage and analysis.

The SXP600 quadrupole mass spectrometer (MS), manufactured by VG Instruments, Inc., was used to conduct the evolved gas analysis (EGA) concurrently with the TGA/DTA runs. This mass spectrometer allows the determination of multiple gas components in the mass range of

TABLE 1

Details of the Catalysts Used in This Investigation

	S, as received (wt%)	S activated, 725°C, 2 h (wt%)	S activated, 650°C, 2 h (wt%)	S.A. (m^2/g)
SO_4^{2-}/ZrO_2	3.92	1.14	2.0	100–120
0.6% $Pt/SO_4^{2-}/ZrO_2$	~4	—	1.84	121 ± 10 (650°C activation)
2% Fe/0.5% $Mn/SO_4^{2-}ZrO_2$	~4	1.36	—	79 ± 10 (725°C activation)

1–300 amu. The mass spectrometer was interfaced to the TGA/DTA unit through a fused silica capillary line, the tip of which was placed at a distance of about 1 in. from the sample. To prevent condensation in the capillary, it was maintained at 170°C by self-resistance heating. The flow rate through the capillary was about 12 ml/min at 170°C. The mass spectrometer has a Vier type-enclosed ion source, a triple mass filter, and two detectors (Faraday cup and a secondary emission multiplier). Data from the mass spectrometer were acquired using a log-historam (LGH) mode, in which the intensities of all peaks in a specified mass range (e.g., 1–100) were monitored and stored repeatedly during the temperature program. A data conversion program was then used to display the intensities of the desired ions as a function of time. In this manner, the changes in the concentration of species in the gas stream can be followed and related through the time scale of the TGA/DTA events.

The Seiko instrument was calibrated for peak temperatures using three standards: Sn, SiO_2, and K_2SO_4. These three standards were run at different rates to calibrate the temperature scale. These data were plotted and fitted to a linear equation, and the peak temperatures for the catalyst samples were corrected using this equation.

In a typical experiment, the sample was heated to 100°C in helium and held there for 1 h. Then the sample was heated to 800°C at a rate of 20°C/min, held there for 10 min, and cooled to 100°C in helium. Soon after the sample was cooled to 100°C, the second gas (air) was introduced. The sample was held at 100°C for 30 min and a second cycle of heating and cooling, similar to the first cycle, began. Thus, the first cycle was run in helium and the second cycle was run in a mixture of He/air (see Fig. 1a).

RESULTS AND DISCUSSION

The composition and surface area of the caalysts used in this study are given in Table 1; analysis of the dried or activated samples, or both, varies slightly from those in Table 1 from batch to batch. It should be noted that in the literature report on TPD experiments (19) with Catalysts I and III, the calcination temperature of catalysts was not given. The report on the synthesis of Catalyst I suggested that 550–600°C is preferred for the best catalytic activity (18). Catalyst I was calcined at 725°C in most experiments, but because calcination temperature may impact catalytic activity adsorption–desorption data were also obtained for a sample calcined at 400°C. The data on CO_2 and SO_2 evolution from all catalysts are summarized in Table 2. In the following, the results of experiments with benzene are presented first, then the results of the study of pyridine, both by TGA and TPD, are shown. A short examination of the nature of the oxidizing agent in the catalysts is then presented.

Reactions with Benzene

In preliminary experiments, Catalysts III, activated *in situ* in the TGA furnace and cooled to 100°C, was exposed for 1 h to benzene vapors by passing He through a benzene bubbler at room temperature. Subsequent heating to 800°C showed no benzene or carbon oxides in the effluent; this failure to adsorb benzene at 100°C is at variance with previous reports (15, 16, 21, 22). However, sample orientation and contact with the flowing vapor are probably responsible for this difference. Therefore, in further experiments all three catalysts were activated at 400°C (or 650°C or 725°C) in a muffle furnace and allowed to cool for 15 min in a desiccator, then quickly transferred to another desiccator, containing liquid benzene, and left there for 25 h. The catalysts gained weight in this process of saturation with benzene. A sample of a catalyst was transferred quickly into the TGA/MS unit and kept there under helium flow at room temperature for 30 min. After excess benzene desorbed and the sample exhibited a constant weight, the temperature program was started.

The TGA/MS data obtained for Catalyst I are shown in Fig. 1. The temperature profile, the DTA, and the weight loss curves are shown in Fig. 1a and the intensity of selected masses of the evolved gases are plotted in Fig. 1b. It is seen that an endothermic weight loss observed in the first step (at room temperature, first 30 min) represents water

TABLE 2
Evolution Temperatures of CO_2 and SO_2 from Catalysts I, II, and III with Preadsorbed Benzene or Pyridine

Sample	CO_2 evolution (°C)		SO_2 evolution (°C)	
	Ads. benzene	Ads. pyridine	Ads. benzene	Ads. pyridine
I (725°C)	400	320	~575	473
	575	473	812	—
	812	—	—	—
II (725°C)	576	610	576	610
	—	~820	818	820
II (650°C)	526	512	526	512
	—	—	812	812
I (400°C)	600	610	600	610
	—	—	640–800	—

and benzene desorption; a further weight loss occurred upon heating to 100°C and this represents an additional loss of water. The water observed when heating to 100°C may be from the instrument as well as the sample. In the third step (heating to 800°C), water (endotherm, m/z 18) desorbed before 200°C and CO_2 (m/z 44) appeared to desorb in three temperature regions, namely 400°C (minor), 580°C, and 812°C (Fig. 1b). Sulfur oxides (m/z 64 and 48) and O_2 (m/z 32) appeared to desorb at 825°C. No benzene (m/z 78) desorbed after the first 30 min at room temperature.

At the end of the run, the sample was cooled to 100°C and the purge gas was switched to the helium/air mixture. After 30 min of equilibration at this temperature, step 3 was repeated. As shown in Fig. 1b, the carbon (coke) left on the catalyst is oxidized to CO_2 but no other masses were observed during this second heating.

The results for reaction of benzene on Catalyst I activated at 400°C are shown in Fig. 2. Because the calcination temperature was too low to induce crystallization of ZrO_2, an exotherm appears in the benzene DTA at the crystallization temperature (612°C). All CO_2 desorbs in one temperature region (instead of three regions in Fig. 1b), centered at 575°C. Furthermore, SO_2 is evolved in a broad range, roughly between 500 and 830°C.

The TGA/MS data obtained from Catalyst II with benzene are presented in Fig. 3 (the first 30 min at room temperature is omitted). Three weight loss regions were observed: desorption of water below 200°C, desorption of both CO_2 and SO_2 centered at 576°C, and desorption of

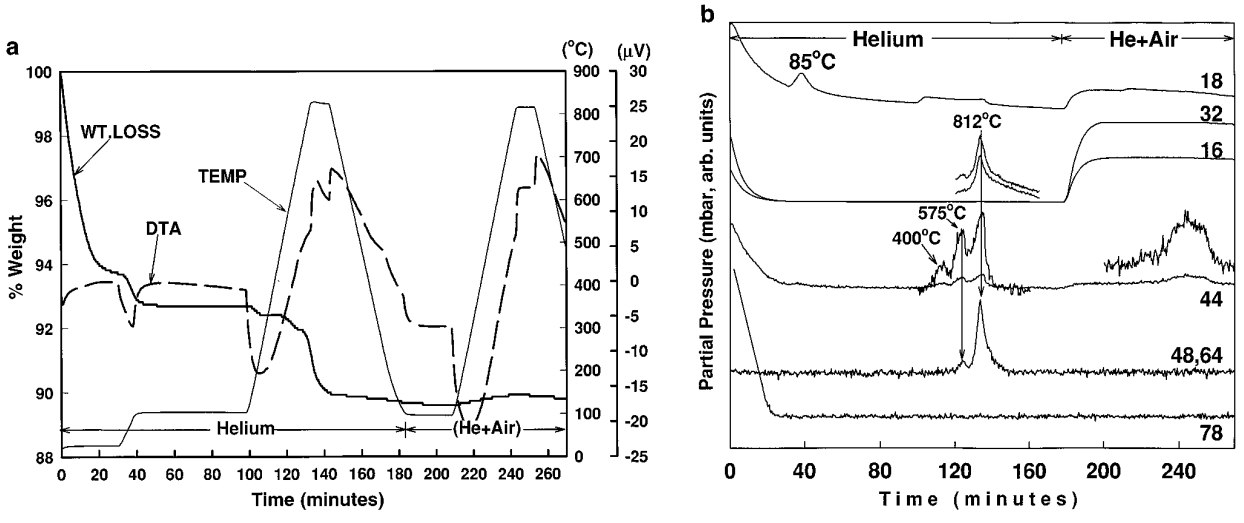

FIG. 1. (a) The weight loss, DTA curves, and the temperature profile plotted against time for heating and cooling the SO_4^{2-}/ZrO_2 catalyst (I) (activated at 725°C for 2 h and saturated with benzene at room temperature) in He, then heating in air. (b) The evolved gas analysis data for the experiment in (a) (mass numbers are indicated for each curve).

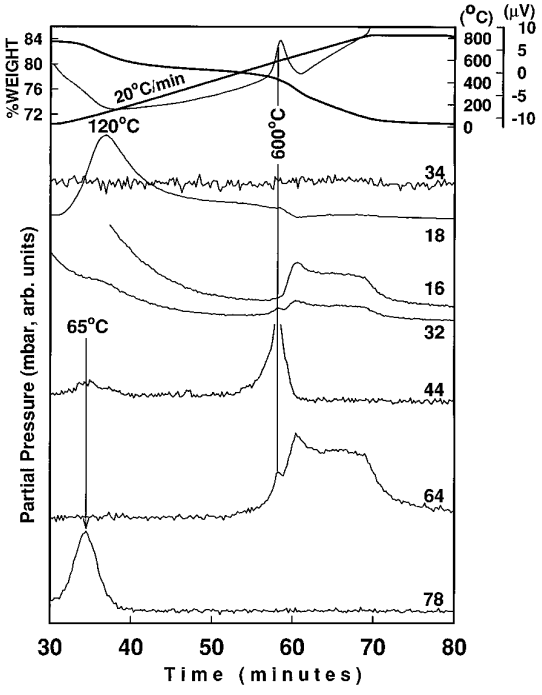

FIG. 2. The evolved species, weight loss, and DTA curves during heating in helium of the SO_4^{2-}/ZrO_2 catalyst (I) activated at 400°C for 2 h and saturated with benzene.

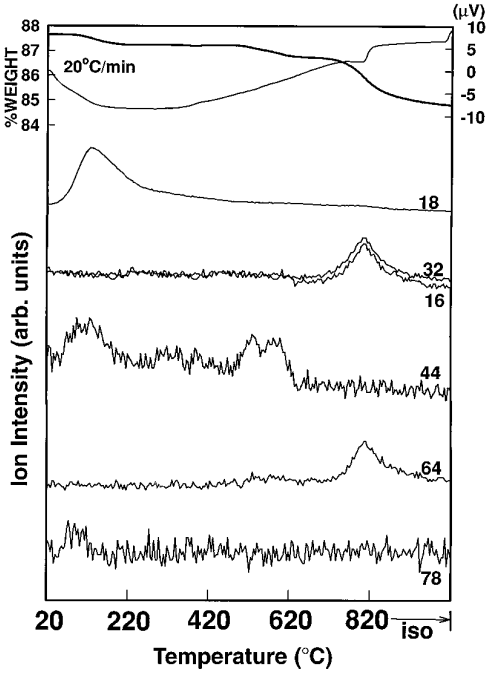

FIG. 3. The evolved species, weight loss, and DTA curves during heating in helium of the $0.6\%Pt/SO_4^{2-}/ZrO_2$ catalyst (II) activated at 725°C for 2 h and saturated with benzene.

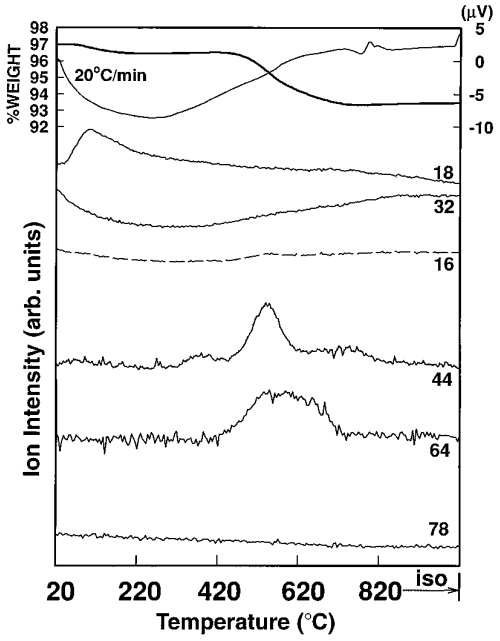

FIG. 4. The evolved species, weight loss, and DTA curves during heating in helium of the $Fe/Mn/SO_4^{2-}/ZrO_2$ catalyst (III) activated at 650°C for 2 h and saturated with benzene.

SO_2 centered at 818°C. The data from Catalyst III (Fig. 4) differed from those of Catalyst II only by a lower temperature of CO_2 desorption (526°C).

A notable difference between Catalyst I and the other two materials is that CO_2 desorbs from I at three temperatures but for II and III only one region of CO_2 desorption is observed. The presence of Fe and Mn reduces the desorption temperature for CO_2. Conversely, the desorption of SO_2 occurs in one temperature region from I, but in two regions from II and III, but the lower temperature for I is very small.

To assess the effect of heating rate upon the results, benzene desorption from Catalysts II and III was also run at 10°C/min heating rate. For Catalyst II, the CO_2 desorption peak and the first SO_2 desorption peak were now seen at 576°C instead of 625°C and the area of the high-temperature (818°C) SO_2 desorption peak was nearly equal to that of the 576°C SO_2 desorption peak. Reaction on Catalyst III was little affected by the heating rate change.

Catalysts II and III were also heated again, this time in air, after the completion of the TGA run in helium, as described for Catalyst I above. Two broad CO_2 (m/z 44) peaks, one beginning around 300°C, the other around 800°C, are observed, unlike for I where only the latter peak had been seen. These results are compared to Fig. 5.

It must be noted that after removal of weakly adsorbed benzene at room temperature, no benzene (m/z 78) was found to desorb in any of the experiments. Benzene is thus

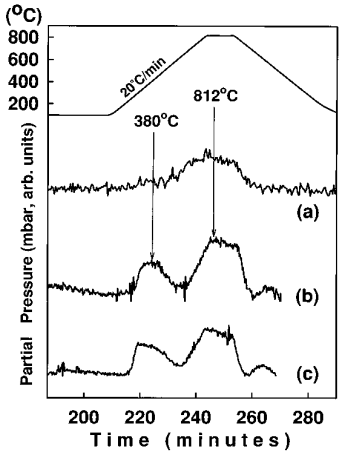

FIG. 5. The m/z 44 (CO_2) peak intensity plotted against time during the second cycle of heatng (in air) of catalysts presaturated with benzene; (a) catalyst (I), (b) catalyst (II), (c) catalyst (III).

converted to CO_2 and coke upon heating of Catalysts I, II, and III in helium and the coke, as expected, is oxidized to CO_2 upon further heating in air.

An attempt was made to monitor the effect of preadsorbing water on the catalyst surface prior to the adsorption of benzene. Three portions of Catalyst II, calcined at 625°C and cooled as described above, were placed in desiccators containing 100% H_2SO_4, 15% H_2SO_4, and water, respectively. These samples, designated as II-A, II-B, and II-C, respectively, were then saturated with benzene and subjected to the TGA/MS experiment as described above. The samples differed in the amount of CO_2 desorbed. Catalyst II-A exhibited a sizeable CO_2 peak at 380°C, a very small one at 810°C, and minor peaks at 400 and 810°C on the second heating in air (coke burning), whereas II-B exhibited very small CO_2 peaks both on TPD and in the coke-burning step and II-C showed virtually no CO_2 desorption. As no benzene peak (m/z 78) was seen in any of these three experiments, it appears that moisture retards or prevents benzene chemisorption (or rather oxidation of physisorbed benzene). The moisture-exposed catalyst was also inactive in hexadecane conversion experiments (26).

Reactions with Pyridine

Catalysts I, II, and III were calcined at 625°C in air, cooled to room temperature in a desiccator, then exposed to pyridine vapors in a desiccator for 25 h, and TGA/MS experiments were conducted as described above for benzene. For Catalyst I, physisorbed pyridine desorption (m/z 79) is centered at 60°C, but a smaller amount of pyridine also desorbs at 320°C (Fig. 6). Water evolution is observed with peaks centered at 60, 100, and 473°C; the latter two peaks are superimposed on a broad continuous background showing some water evolution during the entire heating period. A small amount of CO_2 desorbs at 320°C. At 473°C, sharp peaks corresponding to O, CO_2, and SO_2 are observed indicating that oxidation of pyridine occurs over a narrow temperature range. The intensity of the peak of mass 17 paralleled that of mass 18, indicating that the former was a fragment of water, rather than ammonia. On the other hand, no evidence for evolution of nitrogen oxides appears in the results; the traces NO (m/z = 30) and NO_2 (m/z = 46) do not differ from the background. It is noteworthy that NO, but not NO_2, was clearly observed when dried but uncalcined Catalyst III was heated under helium (decomposition of nitrate salts) (27). Thus, if NO was formed from pyridine over a narrow temperature range for these catalysts, it would have been observed.

Unlike in the experiments with benzene, in the second heating cycle, when the carrier was switched from inert gas to air, very little conversion of coke to CO_2 took place. A broad and weak, almost like an increased background desorption of CO_2, and an equally broad but more intense evolution of water can be observed during heating to 800°C (Fig. 6). Also, no evidence for elution of ammonia, NO, and NO_2 was obtained during the heating in air.

Reaction of pyridine on Catalyst I calcined at 400°C is similar to that on the catalyst calcined at 625°C, except that the total oxidation indicated by evolution of CO_2, SO_2, and O takes place at a higher temperature (600°C

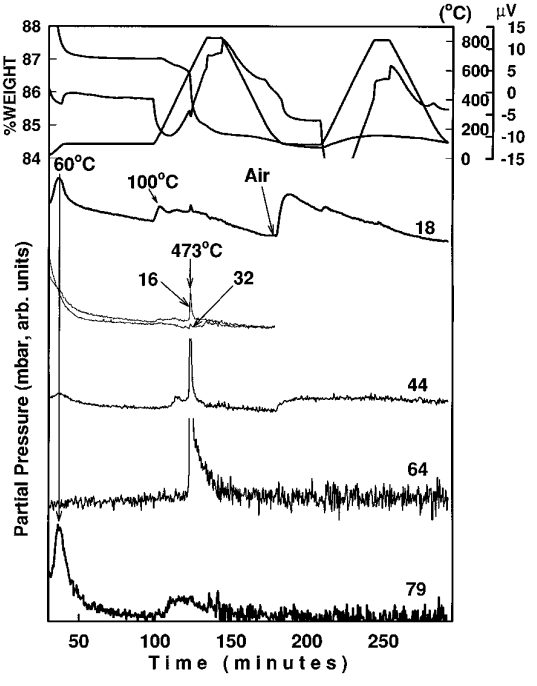

FIG. 6. The evolved species, weight loss, DTA curves, and temperature profile for heating and cooling the SO_4^{2-}/ZrO_2 catalyst (I) (activated at 725°C for 2 h and saturated with pyridine at room temperature) in He, then heating in air.

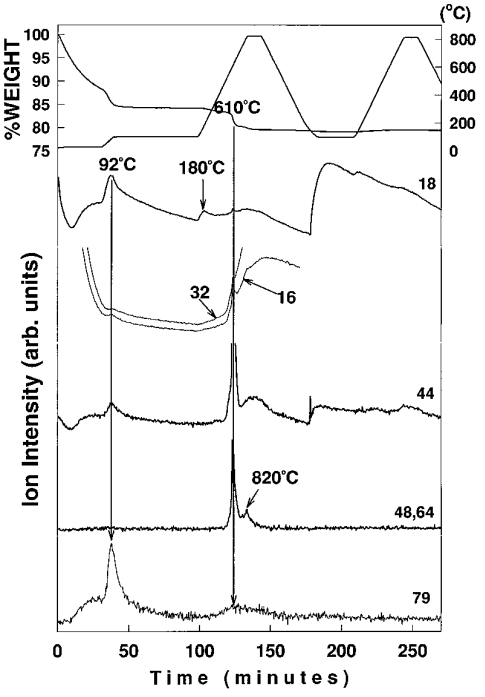

FIG. 7. The evolved species, weight loss, DTA curves, and temperature profile for heating and cooling the 0.6%Pt/SO_4^{2-}/ZrO_2 catalyst (II) (activated at 725°C for 2 h and saturated with pyridine at room temperature) in He, then heating in air.

instead of 473°C from the former), a behavior similar to that observed in the experiments with benzene. Unlike in the benzene experiment, however, no significant CO_2 evolution is seen after the evolution of CO_2 has ended.

The results for Catalyst II are shown in Fig. 7. The weight loss in step 2 (heating to 100°C in helium) was due to evolution of water and pyridine, indicating that physisorbed pyridine is retained more strongly than benzene by this catalyst. A small amount of CO_2 desorbed with pyridine at 92°C. During step 3, a small water peak was observed at 180°C followed by loss of small amounts of water over a more extended period, whereas major amounts of O and O_2, CO_2, and SO_2 desorbed together at 610°C, and a very broad pyridine peak was observed around the same temperature. Smaller amounts of CO_2 and SO_2 desorbed at 820°C. During the oxidation of coke, both CO_2 and water desorbed.

The TGA/MS data for desorption from Catalyst III following pyridine adsorption show that water desorbs at 67 and 180°C (Fig. 8). Following the 180°C peak, water desorbs continuously over a broad temperature range. Pyridine begins to desorb at about 180°C and continues to desorb over the entire temperature range. Major peaks, centered at 512°C, are obtained for CO_2, SO_2, and O, after which SO_2 desorption increases again, attaining a second maximum at 812°C.

Similar behavior was exhibited by pyridine in the TPD experiment with Catalyst III. A peak around 560°C was observed. A sample of the effluent was taken before the entrance into the detector during the peak elution and injected into a GC/MS instrument exhibited m/z 44 (CO_2), 64 and 48 (SO_2), 79 (pyridine, very small), in addition to 28 and 32 resulting mostly from contamination with air in the syringe. It was not possible, therefore, to ascertain from this TPD experiment whether oxygen or nitrogen, or both, resulted from the reaction of the catalyst with pyridine.

These results indicate that pyridine, like benzene, was oxidized on these catalysts, but in this case oxidation was not complete. Some pyridine survived as such, most likely in its hydronated form on the acid centers, and was eluted upon thermal decomposition of the surface ion pair (salt). Another difference is that pyridine reacts with desorption of SO_2 and O_2 at a lower temperature than benzene.

Nature of the Oxidizing Species

Evolution of SO_2 together with or following evolution of CO_2 is a clear indication that the sulfate species on the catalyst surface are responsible for the oxidation of benzene and pyridine. Also, the general pattern for gas evolution during heating of the solid with the preadsorbed substrates is similar for the three catalysts. The temperature at which gas evolution occurs and the number of

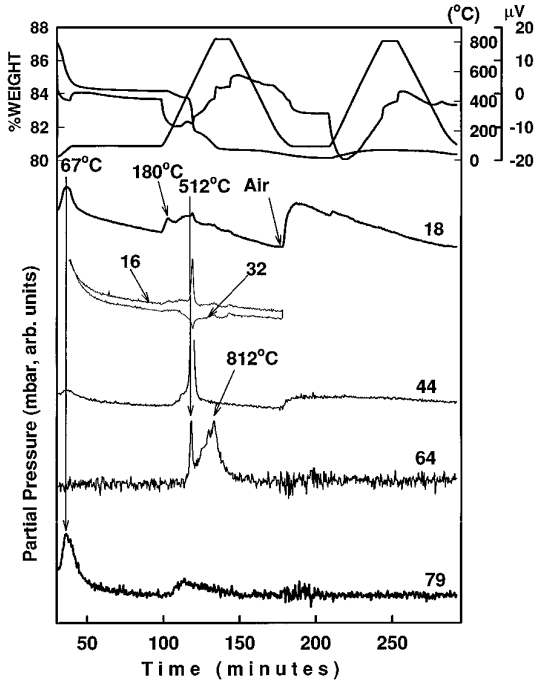

FIG. 8. The evolved species, weight loss, DTA curves, and temperature profile for heating and cooling the Fe/Mn/SO_4^{2-}/ZrO_2 catalyst (III) (activated at 650°C for 2 h and saturated with pyridine at room temperature) in He, then heating in air.

peaks may, however, vary (Table 2). For example, the temperature of CO_2 evolution from adsorbed benzene or pyridine is lower by 50 and 100°C, respectively, for Catalyst III ($Fe/Mn/SO_4^{2-}/ZrO_2$) than for Catalyst II ($Pt/SO_4^{2-}/ZrO_2$). Thus, the metal ions that readily undergo oxidation–reduction cause the oxidation of benzene or pyridine by the adsorbed SO_4^{2-} to occur at lower temperature. In addition, pyridine is oxidized at a lower temperature than benzene is by Catalyst III, but the order is reversed for Catalyst II. The data in Table 2 also show that the presence of Pt or Fe and Mn alters the desorption of products from those obtained from Catalyst I, which was calcined at 400°C, more than from the same type of catalyst, but calcined at 725°C. Therefore, the other components of the solid catalyst have a direct influence upon the oxidizing ability of sulfate.

One final point deserves notice. Both Figs. 1a and 6 show that during the coke oxidation step the weight of the solid increased, even though CO_2 was lost. This suggests that some oxygen from the oxide lattice was consumed for substrate oxidation in the helium atmosphere and heating in air led to restoration of the oxide. An alternative explanation that some reduced sulfur species on the surface was reoxidized is less likely, because similar behavior was obtained for a pure zirconia sample (28).

The mechanism of oxidation of benzene and pyridine on Catalysts I–III was beyond the scope of our investigation. Experiments conducted after the completion of this work indicated that the reaction consists of a one electron transfer from the substrate to the catalyst followed by the trapping of the organic radical cations by the catalyst or their condensation to larger molecules (29). Benzene is adsorbed on the catalyst, and oxidation to heavy products occurs faster than desorption of benzene upon heating. Various metal or metal ion promoters influence the reaction by modifying the one-electron acceptor ability of the sulfated zirconia catalyst. The support and promoters alter the energy of the lowest unoccupied molecular orbital of the sulfate, which accepts the electron from the organic molecule.

CONCLUSIONS

The main reaction occurring upon heating in an inert atmosphere benzene and pyridine adsorbed on sulfated zirconia, Pt-promoted sulfated zirconia, or Fe/Mn-promoted sulfated zirconia is oxidation to carbon dioxide and coking. Formation of sulfur dioxide indicates that sulfate is the oxidizing species. The increase in weight of the solid when the material at the end of the reaction in He is heated again in air, even though the coke is burned off, indicates that some of the oxygen consumed for the oxidation of the organic molecules originates from zirconium oxide.

The data show that the TPD of very weak (benzene) or even stronger (pyridine) organic bases does not measure the acidity of sulfated zirconia or of composite materials based on it. As a general rule, one should establish that no reaction other than hydrogen transfer occurs between the probe base and the surface before trying to use TPD to compare acid strengths of catalysts.

ACKNOWLEDGMENTS

This work was supported by the Commonwealth of Kentucky and the U.S. DOE by Contract DE-AC22-90PC90049. The work at the University of Pittsburgh has been supported by a grant (CTS-9121454) from the NSF. Professors I. Wender and J. Tierney are thanked for the use of their GC-MS instrument.

REFERENCES

1. Tanabe, K., *Mater. Chem. Phys.* **13,** 347 (1985).
2. Nascimento, P., Akratopoulou, C., Oszagyan, M., Coudurier, G., Travers, C., Joly, J. F., and Vedrine, J. C., *Stud. Surf. Sci. Catal.* **75,** 1185 (1993).
3. Hosoi, T., Shimadzu, T., Itoh, S., Baba, S., Takaoka, H., Imai, T., and Yokoyama, N., *Prepr. Am. Chem. Soc., Div. Petrol. Chem.* **33,** 562 (1988).
4. Wen, M., Y., Wender, I., and Tierney, J. W., *Energy Fuels* **4,** 372 (1990).
5. Yamaguchi, T., *Appl. Catal.* **61,** 1 (1990).
6. Yamaguchi, T., Tanabe, K., and Kung, Y. C., *Mater. Chem. Phys.* **16,** 27 (1986).
7. Arata, K., *Adv. Catal.* **37,** 165 (1990).
8. Ebitani, K., Konishi, J., and Hattori, H., *J. Catal.* **130,** 257 (1991).
9. Ebitani, K., Tsuji, T., Hattori, H., and Kita, H., *J. Catal.* **135,** 609 (1992).
10. Ebitani, K., Konno, H., Tanaka, T., and Hattori, H., *J. Catal.* **135,** 60 (1992).
11. Ebitani, K., Konno, H., Tanaka, T., and Hattori, H., *J. Catal.* **143,** 322 (1993).
12. Sayari, A., and Dicko, A., *J. Catal.* **145,** 561 (1994).
13. Zhao, J., Huffman, G. P., and Davis, B. H., *Catal. Lett.* **29,** 385 (1994).
14. Zhang, C., Miranda, R., and Davis, B. H., *Catal. Lett.* **29,** 349 (1994).
15. Bensitel, M., Saur, O., and Lavalley, J. C., *Mater. Chem. Phys.* **17,** 249 (1987).
16. Other papers on this subject are cited in Ref. (14).
17. Hollstein, E. J., Wei, J. T., and Hsu, C.-Y., U.S. Patents 4,918,041 (1990), and 4,956,519 (1990).
18. Hsu, C.-Y., Patel, V. K., Vahlsing, D. H., Wei, J. T., and Myers, H. K., Jr., U.S. Patent 5,019,671 (1991).
19. Lin, C.-Y., and Hsu, C.-Y., *J. Chem. Soc., Chem. Commun.* **20,** 1479 (1992).
20. For the use of PhH to assess zeolite acidity; see Choudhury, V. R., Srinivasan, K. R., and Singh, A. P., *Zeolite* **10,** 16 (1990).
21. Fărcaşiu, D., Fisk, S. L., Melchior, M. T., and Rose, K. D., *J. Org. Chem.* **47,** 453 (1982).
22. Fărcaşiu, D., Marino, G., Miller, G, and Kastrup, R. V., *J. Am. Chem. Soc.* **111,** 7210 (1989) and references therein.
23. Spiro, T. G., and Fărcaşiu, D., unpublished.

24. Fărcaşiu, D., Presented at the Symposium on Surface Science of Catalysis, Strong Solid Acids, 1993, Abstract COLL 211, 206th ACS National Meeting, Chicago, IL.
25. Jatia, A., Chang, C., Macleod, J. D., Okubo, T., and Davis, M. E., *Catal. Lett.* **25,** 21 (1994).
26. Keogh, R. A., Srinivasan, R., and Davis, B. H., *J. Catal.* **151,** 292 (1995).
27. Srinivasan, R., Keogh, R. A., and Davis, B. H., *Appl. Catal*., in press.
28. Srinivasan, R., Watkins, T. R., Hubbard, C. R., and Davis, B. H., *Chem. Mater.* **7,** 725 (1995).
29. (a) Ghenciu, A., Li, J. Q., and Fărcaşiu, D., Presented at the 14th North American Meeting of The Catalysis Society, Snowbird, UT, June 12, 1995, Abstract T. 51; (b) Ghenciu, A., and Fărcaşiu, D., paper in preparation.